**Joint Pathology Center**
**Veterinary Pathology Services**

# WEDNESDAY SLIDE CONFERENCE
# 2020-2021

# Conference 18

**10 February, 2021**

Joint Pathology Center
Silver Spring, Maryland

---

## CASE 1: 17N00143 (4117640-00)

**Signalment:**
16-year-old, castrated male, Brittany Spaniel, *Canis familiaris*, dog

**History:**
In June 2013 the animal was diagnosed via echocardiogram by an outside cardiology service with a right atrial mass that appeared to originate from the atrial septum, initially the mass measured approximately 1.5 cm in diameter. The animal was evaluated yearly by a cardiologist and at his most recent appointment in July 2016, the mass was noted to be taking up 80% of his right atrium. Before the diagnosis of the atrial mass and through the course of his disease, the animal had a history of ventricular arrhythmia, paroxysmal atrial tachycardia and mild pulmonary hypertension. Eight months after his last appointment with the referral cardiologist the animal stopped eating, became lethargic, was vomiting and coughing. He presented to his primary care veterinarian where he was found to have fluid in his abdomen. The animal was humanely euthanized and presented to UW Veterinary ER service for necropsy.

**Gross Pathology:**
On gross examination, there was a multilobulated, pink-tan to red, semi-firm mass extending from the endocardial surface of the right atrium measuring approximately 7.0 x 8.0 x 3.5 cm. There was a single separate dark red to black nodule on the endocardial surface at the base of the right atrial appendage, which measured 0.9 x 0.7 x 0.5 cm. A mass with a necrotic center was also present in the left ventricular wall measuring 14 mm in diameter. On cut section, all masses were mottled pale tan to dark red. Additionally there was a focal area of pink to tan discoloration and contracture on the papillary muscle of the left ventricle measuring 0.9 x 0.7 cm. The heart weight 253.4 grams corresponding to approximately 1.7% of the body weight.

**Laboratory results:**
None.

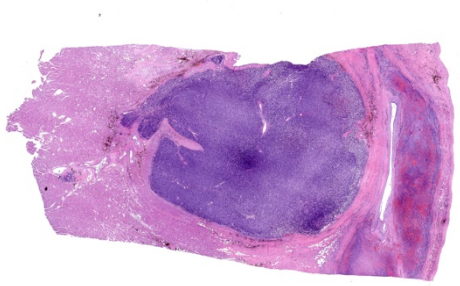

*Heart and great vessels, dog. There is a large neoplasm infiltrating the myocardium, great vessels, and adjacent fibrovascular tissue of presumably the heart base. (HE, 6X)*

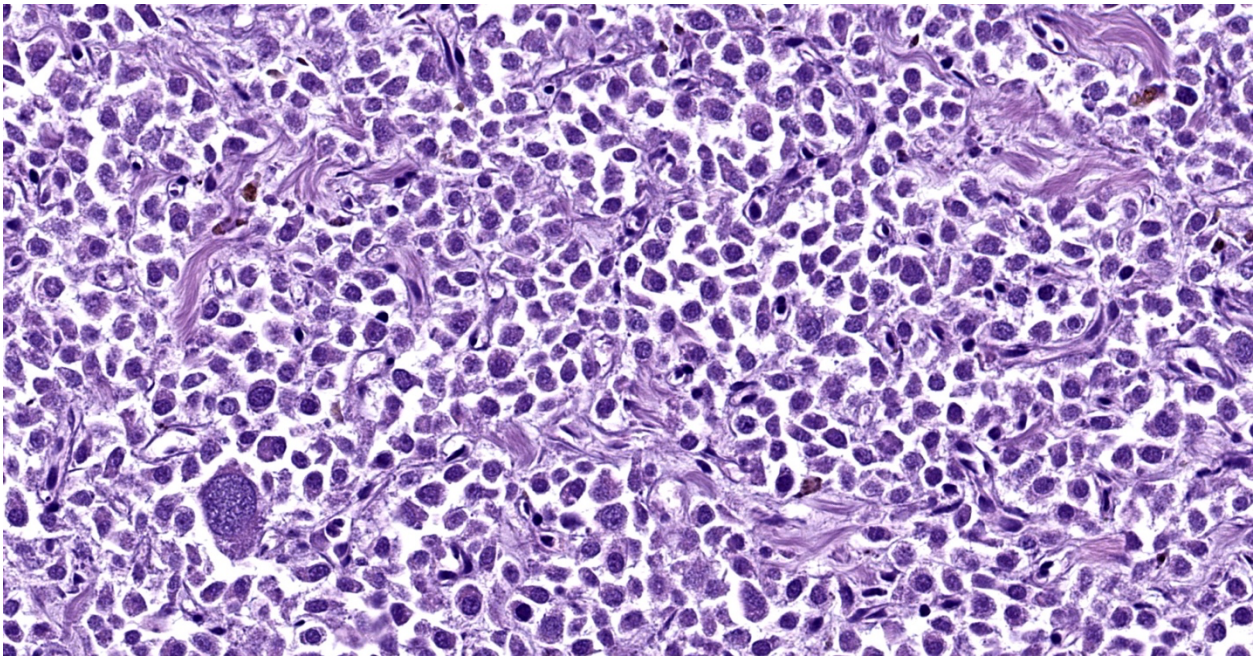

*Heart and great vessels, dog. Neoplastic cells are arranged in nest and packets and have moderate amounts of granulated cytoplasm, round nuclei with indistinct nuclei, and occasionally cells with enlarged, pleomorphic nuclei (lower left). (HE, 400X)*

**Microscopic description:**

*Right atrium:* An unencapsulated, moderately well demarcated and moderately cellular neoplasm multifocally infiltrates, expands and effaces the myocardium. The neoplastic cells are arranged in nests, packets and small lobules and are supported by a fine fibrovascular stroma. The cells are round to polygonal with variably distinct cell borders, moderate amounts of finely granular amphophilic cytoplasm and round nuclei with coarsely clumped chromatin and indistinct nucleoli. The cells exhibit moderate to marked anisocytosis and anisokaryosis and mitotic figures are present (0-3 mitotic figures per 400x field). Occasional neoplastic cells have large, multilobed nuclei. There are multifocal to coalescing areas of necrosis throughout the mass. Neoplastic cells multifocally occupy and occasionally expand the lumens of blood vessels within the surrounding myocardium. Areas of hemorrhage, fibrosis and hemosiderin-laden macrophages multifocally surround the neoplasm.

**Contributor's morphologic diagnosis:**

Right atrium (per submitter), atrial paraganglioma

**Contributor's comment:**

Cardiac tumors are relatively uncommon in the canine population.[1,4,14,23] The most common type of cardiac tumor is hemangiosarcoma follow by paragangliomas occurring at the heart base (i.e. chemodectomas, also known as aortic body tumors), lymphoma and ectopic thyroid carcinoma.[4,15,23]

Paragangliomas are neuroendocrine tumors that originate from chromaffin cells that are associated with sympathetic ganglia (for example

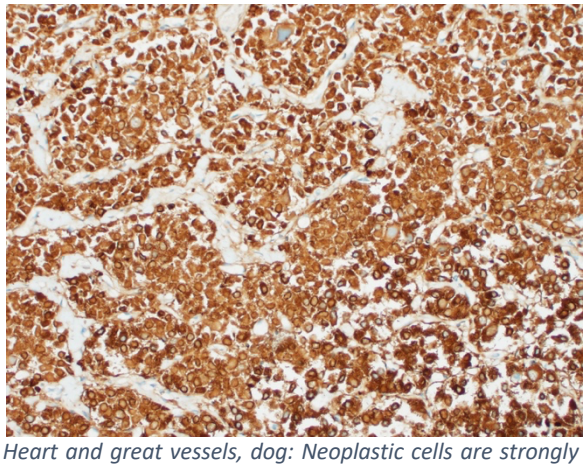

*Heart and great vessels, dog: Neoplastic cells are strongly immunopositive for synaptophysin (anti-synaptophysin, 400X)*

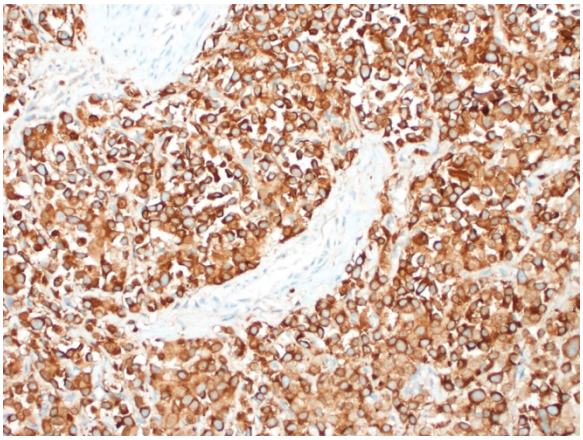

*Heart and great vessels, dog: Neoplastic cells are strongly immunopositive for chromogranin A (anti-chromagranin A, 400X)*

adrenal medulla pheochromocytoma) or the parasympathetic ganglia (for example aortic body / chemodectoma).[8,11,17]

Paraganglia are groups of chromaffin neurosecretory cells of neural crest origin located around ganglia that are dispersed throughout the body.[5] They are classified as sympathetic or parasympathetic according to their location and neural association.[5,7] Sympathetic paraganglia, of which the adrenal medulla is the prime example, are distributed along paravertebral sympathetic chains and nerves that innervate cervical, thoracic, retroperitoneal and pelvic organs.[5,7,11] Parasympathetic paraganglia, also referred to as chemoreceptors, are distributed primarily along the cervico-thoracic branches of the glossopharyngeal and vagus nerves and include the orbital, vagal, laryngeal, and subclavian paraganglia, as well as the carotid and aortic bodies.[5,7,11]

The unifying feature of sympathetic paragangliomas is the fact that they can be functional and are able to synthesize and secrete significant amounts of catecholamines,[7,8,17] whereas parasympathetic paragangliomas tend to be non-functional and don't release catecholamines or if they do, they tend to release dopamine so human or animal patients usually do not present with typical symptoms of catecholamine excess such as systemic hypertension or tachycardia.[8,17,18] In veterinary medicine, the most common parasympathetic tumor is the chemodectoma, also known as aortic/carotid tumor or non-chromaffin paraganglioma.[4,15,16] However, the latter term is an antiquated and confusing term, considering that all types of paraganglia tumors originate from chromaffin cells and that approximately 40-50% of the parasympathetic tumors are recognized to secrete catecholamine metabolites (such as dopamine) to some extent.[17]

In human medicine, 95% of all reported sympathetic paragangliomas are pheochromocytomas. Only 2% occur above the diaphragm, which account for 0.3% of all mediastinal/ cardiac neoplasms, and less than 50% of those tumors are functional. In veterinary medicine, the distribution and functionality are very similar.[19] Pheochromocytomas are the most common neoplasia arising from the adrenal medulla, they are infrequently functional, and there are only rare case reports of sympathetic cardiac paraganglioma of which two were located in the right atrium and one in the left atrium.[2,4,21,23] In contrast, chemodectomas, which were mentioned previously, are the second most common parasympathetic cardiac paraganglioma.[4,12,15] The distinction between sympathetic or parasympathetic cardiac tumors should be mainly based on location since there are no consistent histologic differences between them.[8,17] Chemodectomas are typically located on the epicardial surface of the heart base along the aortic body or atria and occasionally extend to the atria, or the interatrial septum. Sympathetic cardiac paragangliomas are generally located within the atria along the atrioventricular sulcus and near the roots of the great vessels,[4,7,8,17,20] as in this case.

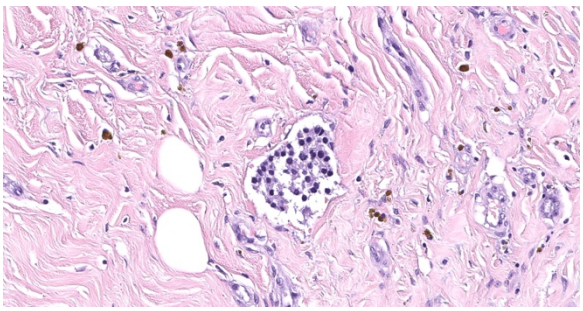

*Heart and great vessels, dog: Neoplastic cells are present within vessels in the adjacent vessels. (HE, 400X)*

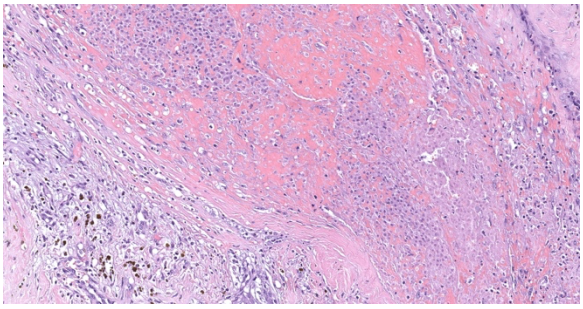

*Heart and great vessels, dog: There are areas of vascular invasion with necrosis, hemorrhage, siderophage accumulation, and fibroplasia. (HE, 400X)*

In general, paragangliomas are composed of tumor cells containing intracytoplasmic hormonal secretory granules which are revealed with an argyrophil reaction, such as Grimelius's methods. The neoplastic cells are typically arranged in nests or packets, known as a Zellballen pattern, and are surrounded by sustentacular cells.[4,11,13,17,20] Giant neoplastic cells with bizarrely shaped, multilobed, densely basophilic nuclei are often seen.[4,8] Immunohistochemically, they are positive for chromogranin, synaptophysin and neuron specific enolase (NSE). Ultrastructurally, both adrenalin- and noradrenalin-type granules are demonstrated in the cytoplasm of the neoplastic cells.[3,11,13,22]

In this case, the tumor developed within the right atrium, extended to the right atrial appendage, and left ventricular wall without involvement of the epicardial surface or the aortic body. Neoplastic cells exhibited the characteristic Zellballen pattern and stained positively for chromogranin A and synaptophysin. Although definitive testing was not performed to confirm the functionality of this tumor (urine catecholamine metabolite quantification for example) we suspect that this tumor was a functional sympathetic atrial paraganglioma based on location, histopathology, immunohistochemistry and classical catecholamine associated clinical signs (systemic hypertension and tachycardia); however, generalized cardiac dysfunction could account for the clinical signs of systemic hypertension and tachycardia.

In conclusion, we believe this is a great case to encourage the review of the classification and distribution of normal paraganglia as well as the appropriate name for neuroendocrine neoplasms arising within or near the heart base.

**Contributing Institution:**
University of Wisconsin
School of Veterinary Medicine
Madison, WI
https://www.vetmed.wisc.edu/departments/pathobiological-sciences/

**JPC diagnosis:**
Heart and great vessels: Paraganglioma (neuroendocrine carcinoma).

**JPC comment:**
The contributor provides a concise summary of these neoplasms. In human medicine, research has progressed to more advanced stages than in veterinary medicine, with the identification of approximately 40% of pheochromocytomas and paragangliomas associated with germline pathogenic variants in 12 known susceptibility genes. Patients identified with the most increased risk have heterozygous pathogenic variations of *SDHD*, with primarily paternal transmission to offspring. This *SDHD* variation accounts for approximately 9% of all pheochromocytomas and paragangliomas. Succinate dehydrogenase (SDH) complex is part of the mitochondrial respiratory pathway and plays a key role in the Kreb's cycle.[6] In veterinary medicine, there has been loose association of chemodectoma and brachycephalic breeds of dogs. Proposed mechanisms have been related to oxygen tension,[4] but a heritable trait unrelated to oxygen tension should not be discounted, as these breeds have been grossly manipulated over time.

Various treatments in canine patients with chemodectoma have been documented. While recent studies suffer from low statistical power, a study in six dogs with chemodectoma had measurable decrease in tumor volume following stereotactic body radiation, with a likely increased survival time.[10] On the other hand, a retrospective study of dogs with chemodectoma and treated with toceranib (Palladia) showed no significant change in survival.[9] While these early

results will likely shape future treatment for this tumor type, caution should be exercised in extricating statistical meaning from these studies with small sample sizes.

During conference discussion, the moderator emphasized the importance of clinical history and gross pathology to help make the diagnosis in these cases. In this case, the neoplasm was likely functional, and was arising from the endocardial surface of the right atrium, making chemodectoma a less likely diagnosis.

**References:**


1. Aupperle H, Marz I, Ellenberger C, Buschatz S, Reischauer A and Schoon HA. Primary and secondary heart tumors in dogs and cats. *J Comp Path*. 2007;136:18-26. 876
2. Buchanan, J. W., Boggs, L. S., Dewan, S., Regan, J. and Myers N. C. Left atrial paraganglioma in a dog: echocardiography, surgery, and scintigraphy. *J. Vet. Intern. Med*. 1998; 12: 109-115.
3. Brown PJ, Rema A, Gartner F. Immunohistochemical characteristics of canine aortic and carotid body tumors. *J Vet Med.* 2003;50:140.
4. Capen CC. Tumors of the endocrine glands. In: Meuten DL, ed. *Tumors in Domestic Animals*. 5th ed. Ames, IA: lowa State Press; 2016: 828-833.
5. DuBray M.M, La Perle C, Jordan D. Endocrine System. In: M Piper. Dintzis T, Dintzis S.M. Comparative Anatomy and Histology: A Mouse and Human Atlas. 2012, Pages 211-227
6. Fishbein L. Pheochromocytoma/ Paraganglioma: Is this a Genetic Disorder? *Current Cardiology Reports*. 2019;21:104.
7. Fishbein L, Leshchiner I, Walter V, Pacak K, Nathanson K.L, Wilkerson M.D. Comprehensive Molecular Characterization of Pheochromocytoma and Paraganglioma. *Cancer Cell*. 2017; 31: 181-193.
8. Lam A.K. Update on Adrenal Tumors in 2017 World Health Organization (WHO) of Endocrine Tumors. *Endocrine Pathology*. 2017; 3: 213-227
9. Lew FH, McQuown B, Borrego J, Cunningham S, Burgess KE. Retrospective evaluation of canine heart base tumours treated with toceranib phosphate (Palladia): 2011-2018. *Veterinary and Comparative Oncology*. 2019;17(4):465-471.
10. Magestro LM, Gieger TL, Nolan MW. Stereotactic body radiation therapy for heart-base tumors in six dogs. *Journal of Veterinary Cardiology*. 2018;20(3):186-197.
11. Moonim M.T. Tumours of chromaffin cell origin: phaeochromocytoma and paraganglioma. *Diagnostic Histopathology*. 2012; 18: 234-244.
12. Rizzo SA, Newman SJ, Hecht S. Thomas WB. Malignant mediastinal extra-adrenal paraganglioma with spinal cord invasion in dog. *J Vet Diagn Invest*. 2008; 20:372-375.
13. Romanucci M, Malatesta D. Cytological, histological and ultrastructural nuclear features of monster cells 151:57-62. in canine carotid body carcinoma. *J Comp Path*. 2014;
14. Robinson W.F, Robinson N.A. Cardiovascular system. In: Maxie MG, ed. Jubb, Kennedy, and Palmer's Pathology of Domestic Animals. Vol 3. 6th ed. Philadelphia, PA: Saunders Elsevier; 2016:52-54.
15. Rosol T, Grone A. Endocrine glands. In: Maxie MG, ed. Jubb, Kennedy, and Palmer's Pathology of Domestic Animals. Vol 3. 6th ed. Philadelphia, PA: Saunders Elsevier; 2016:354-356.
16. Patnaik A.K, Erlandson R.A, Lieberman P.H. Extra-adrenal pheochromocytoma (paraganglioma) in a cat. *J Am Vet Med Assoc*. 1990; 197:104-106v
17. Stephanie M, Fliedner M.J, Brabant B, Lehnert H, Pheochromocytoma and paraganglioma: genotype versus anatomic location as determinants of tumor phenotype. *Cell Tissue Res*. 2018; 372:347-365.
18. Tischler, A. S. Pheochromocytoma and extra-adrenal paraganglioma: updates. *Arch. Pathol. Lab. Med.* 2008; 132: 1272-1284.
19. Turley AJ, Hunter S, Stewart MJ. A cardiac paraganglioma presenting with atypical chest pain. *Eur J of Cardio-Thoracic Surg*, 2005. 28:352-354
20. Treggiari E, Pedro B, Dukes-Mc Ewan J, Gelzerand A.R, Blackwoo L. A descriptive review of cardiac tumors in dogs and cats. *Veterinary and Comp. Onco*. 2015; 15: 273-288.
21. Wey, A. C. and Moore, F. M. Right atrial chromaffin paraganglioma in a dog. *J. Vet. Cardiol*. 2012; 14: 459-464.
22. Yamamoto S, Fukushima R. Histopathological and Immunohistochemical evaluation of malignant potential in canine aortic body tumours. *J Comp Path*. 2013; 149:182-191.

23. Yanagawa H, Hatai H, Taoda T, Boonsriroj H, Kimitsuki K, Park C. Canine Case of Primary Intra-Right Atrial Paraganglioma. *J. Vet. Med. Sci*. 2014 76(7): 1051-1053.

---

**CASE 2: MK18-01471 (4117513-00)**

**Signalment:**
19-year-old, female, Rhesus macaque (*Macaca mulatta*)

**History:**
19-year-old female rhesus macaque with a history of anorexia, increased respiratory effort, swelling of the extremities and neck. Thoracic radiographs revealed an enlarged rounded heart which occupied the majority of the thoracic cavity. On auscultation, lung fields had wheezes and crackles. The heartbeat was faint. Due to the poor prognosis the macaque was euthanized.

**Gross Pathology:**
Examination revealed moderate subcutaneous edema involving the arms, legs and trunk. The macaque was obese with excessive body fat present. Approximately 200 ml of clear fluid was present in the abdomen with approximately 100 ml of similar fluid in the thorax. The heart was severely enlarged with severe dilatation of the right ventricle. The heart weighed 55 grams (0.04 % of body weight). There was excessive epicardial fat present, especially along the surface of the right ventricle. The wall of the right ventricle revealed large areas with little or no visible cardiac muscle. The left ventricle was small in profile compared to the extremely dilated right ventricle. The left ventricular free wall measured 0.6 cm, septum 0.5 cm, right ventricular free wall not including adjacent adipose tissue was 0.15 cm and with adjacent adipose tissue 0.45 cm. Sections of lung were atelectatic and had multifocal, up to 3-4 mm diameter, slightly raised gray to tan foci consistent with lung mite lesions. The liver was enlarged with rounded edges and was tan to brown with a lobular pattern, consistent with chronic passive congestion. A mass was present involving the body of the uterus which measures 3.5 x 3.5 x 4.0 cm. No other gross abnormalities were noted.

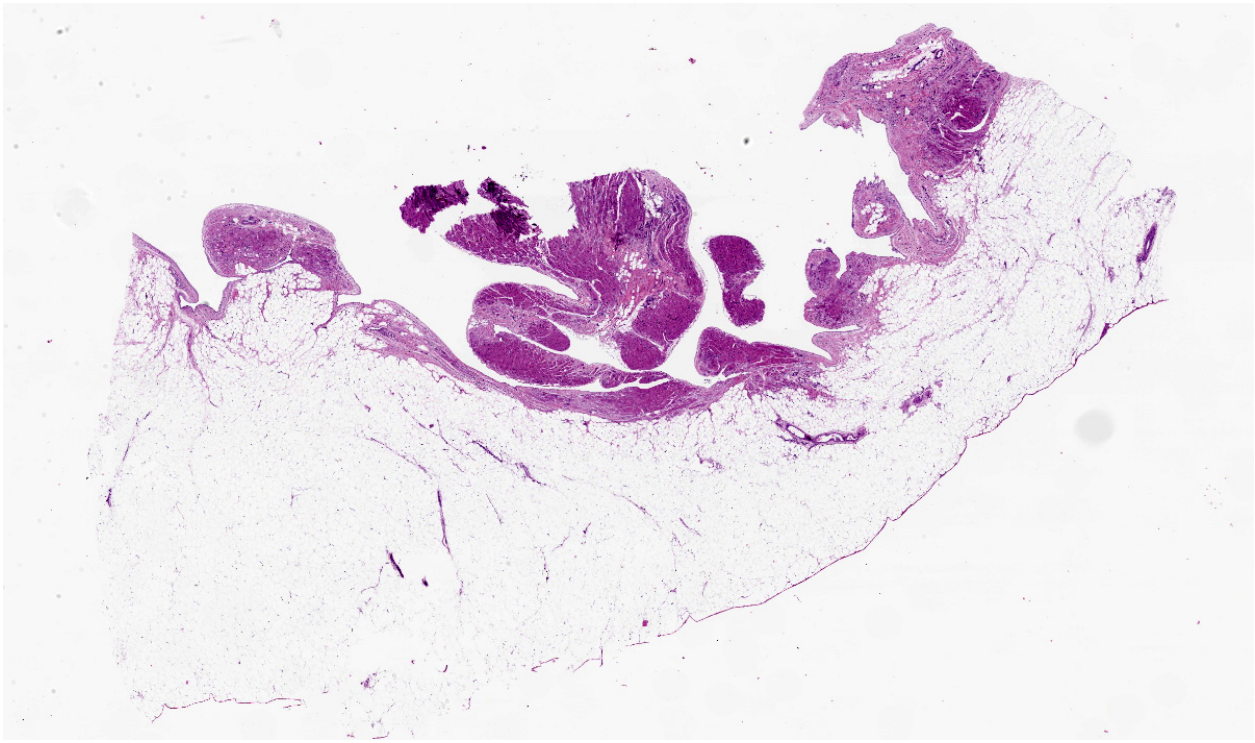

*Heart, right ventricle, rhesus macaque. Subgross magnification of a submitted section of right ventricle in which the myocardium is almost totally replaced by mature adipocytes. (HE, 5X)*

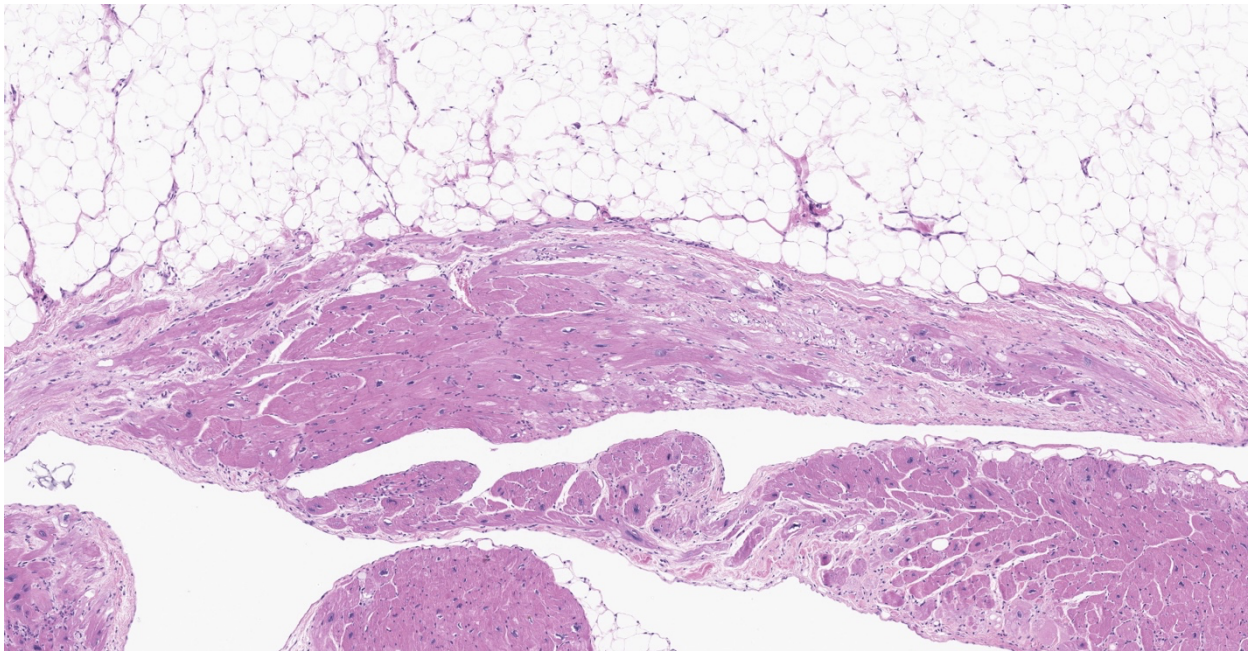

*Heart, right ventricle, rhesus macaque. At the advancing edge of infiltrating adipose tissue, there is myofiber atrophy, loss, and interstitial fibrosis. (HE, 60X)*

**Laboratory results:**
None.

**Microscopic description:**
Heart: There is severe infiltration of adipose tissue within the wall of the right ventricle with severe atrophy and loss of myocytes. Remaining myocytes are hypertrophied with karyomegaly. Interstitial fibrosis is present adjacent to areas of existing myocytes and adjacent adipocytes. Focal mild to moderate fibrosis is noted in the interventricular septum. The left ventricle is unremarkable.

Other tissues: Liver: Scattered centrilobular regions are congested with pericentral necrosis evident (consistent with chronic passive congestion). There is moderate to severe periportal to midzonal lipidosis. Prominent pulmonary bronchiectasis with associated lung mites and peribronchiolar lymphoplasmacytic infiltrates were noted in the lung. The large uterine mass was a leiomyoma.

**Contributor's morphologic diagnosis:**
Rhesus macaque (*Macaca mulatta*) heart, cardiomyopathy, dilatative, right sided, severe with marked adipose deposition and myocyte atrophy. Fibrosis, interatrial septum and right ventricle and septum

Liver: Centrilobular necrosis and congestion
Liver: lipidosis, moderate to severe with centrilobular necrosis.

**Contributor's comment:**
Arrhythmogenic right ventricular cardiomyopathy (ARVC) was first reported in four male human patients in 1978 in France documenting clinical symptoms and EKG data. These patients experienced tachycardia with no prior clinical history, unusual right side QRS, S-T and conduction abnormalities. A subsequent report in 1982 included a study in which patients had right sided ventricular tachycardia along with decreased conduction by EKG. These patients presented with hypokinesis with localized dyskinesia. The histology revealed fatty infiltrates and fibrosis in cardiac tissue.[11] Of twenty-two human athletes who died while participating in sports including soccer, long distance running, swimming and running, ARVC was found to be the cause of death in six cases.[4]

ARVC is a genetic disease linked to defects in 13 different genes that are vital components of the intercalated disc. In 50% of cases a familial

genetic link can be identified leaving researchers to believe that other genes may be involved in this cardiomyopathy or that it may occur spontaneously. The first genetic link was reported in 1990 in which family history revealed a genetic mutation inherited at a higher ratio in males with variable penetrance and expression. This genetic autosomal dominant cardiomyopathy effects 1:2,000-5,000 people, typically RAeD diagnosed in 20-40-year-olds with predilection in males. In 50% of cases the most common symptom is sudden death while exercising.[13]

Most cases of ARVC are caused by functional mutations to ion channels, accessory proteins or structural genes. The intercalated disc has three components, the gap junction, the desmosome and the adheren junction, that function to keep the heart beating rhythmically. The gap junction is formed when connexins from two individual cells join making a channel. The connexins are made of six equal subunits who role is to move ions, sugar molecules, amino acids and nucleotides through the channel to synchronize the electrical potential of the two cells. A gene mutation of connexin 43 reduces the number of sodium channels subsequently creating a delay in repolarizing myocytes. This defect does not allow an adequate influx of Na+ leading to asynchronous beating of myocytes and eventual arrhythmias.[15,18] The desmosome (macula adherens) provides structural support utilizing the intermediate filaments from neighboring cells. The desmosome has two structural parts, armadillo controlled by the JUP gene and plakins. Two proteins, desmoplakin and plakophilin exists in two adhesion states controlled by the amount of calcium. The plakins anchor the intermediate filaments. A defect found in ARVC to plakophilin 2 or desmoplakin weakens the bond with the intermediate filaments. The adherens junction provides strength, stability and adhesion between myocytes forming the bond between desmoglein and desmocollin in the intracellular space. It is formed by cadherins or laminins which form calcium dependent adhesions that also control cell fate, transduces signals and has other embryological roles. Defects in desmoglein 1, 2 and 4 and desmocollin 2 lead to weakening of the adherens junction and subsequent loss of function. It is this loss of function of the adherens junctions that cause remodeling of the

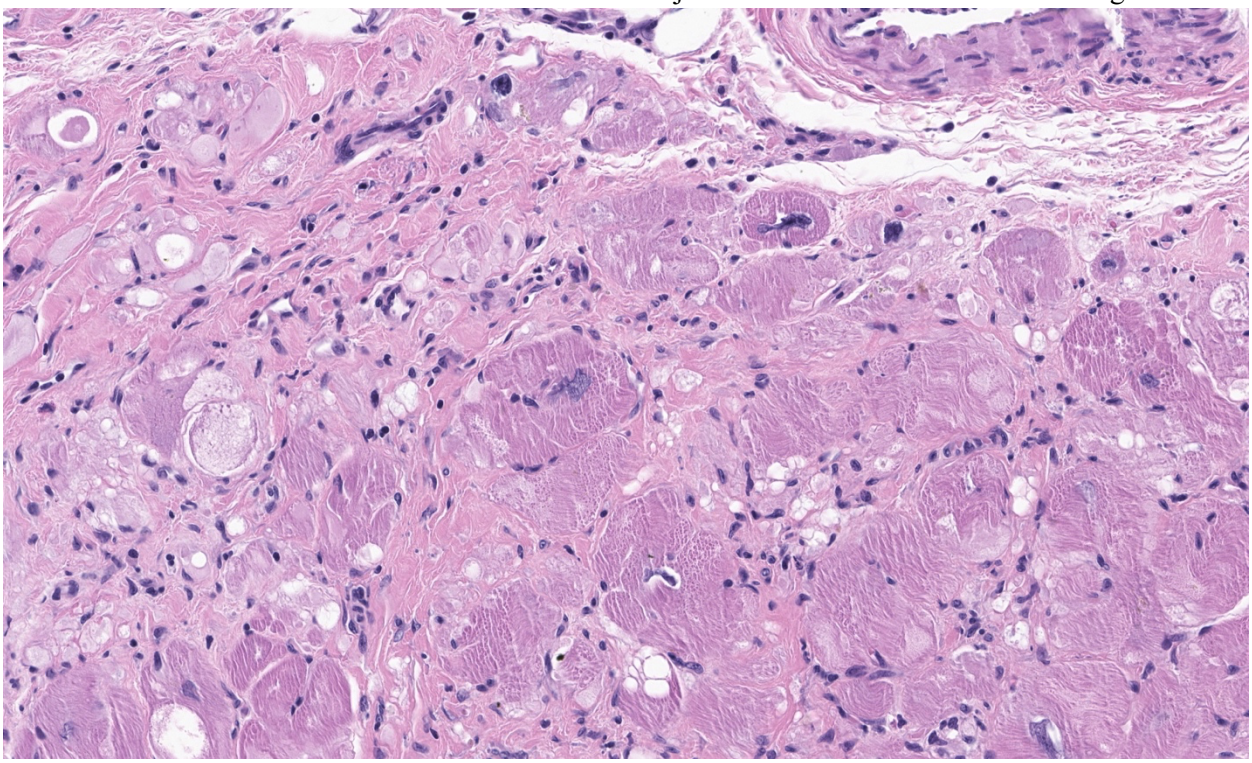

*Heart, papillary muscle, rhesus macaque. Remaining cardiomyocytes exhibit cytoplasmic vacuolation, loss of cross-striations, atrophy and nuclei are karyomegalic and pleomorphic. There is replacement fibrosis in areas of myofiber loss. (HE, 253X)*

intercalated disc, poor adhesion, apoptosis and fibrofatty replacement.[5]

The most common symptoms with ARVC are syncope, palpitations, chest pain and arrhythmias. Diagnosis is by unique EKG patterns that include repolarization and depolarization abnormalities and ventricular arrhythmias. Often the first sign of disease is sudden death. Definitive diagnosis is from family history, EKG and biopsy. Dilation is evident by ultrasound in the right ventricle. Histology reveals degenerating myocytes, some residual myocytes and replacement with adipose or fibrous tissue that may be transmural. Often trapped myocytes are seen along with an inflammatory response in the right ventricle with thinning of the ventricular wall.[16]

Reports of ARVC have been documented in boxer dogs, a Siberian husky, a Weimaraner, cats and horses.[6,7,9,10,12] The boxer dogs did not show signs of illness until the age of six with abrupt onset. As with humans, dogs that led the most sedentary lifestyle showed slower disease progression. The dogs that exercised most as with the human endurance athletes, were at greatest risk for sudden death. Genetic testing of the 49 dogs for striatin, which is instrumental in the formation of desmosomes revealed 33 had a gene mutation. Weakness to desmosomes can have both mechanical and electrical implications causing myocyte failure and arrhythmias due to poor conduction and cell to cell adhesion. The thinner wall of the right ventricle is unable to withstand the stress generated by exercise due to defects in cell to cell adhesion of myocytes.[1]

Two cats case histories documented ACRV in which both cats presented with pleural effusion, rapid breathing and an echocardiogram that revealed a very enlarged right ventricle and atrium. Histology of one cat heart revealed right ventricular dilation, fibrous and adipose replacement of myocytes, entrapped myocytes and inflammation. There was transmural fat replacement.[10]

Two horses' sudden death was investigated one occurring shortly after strenuous exercise. Grossly both hearts were gelatinous, and one had an area measuring 2 cm x 6 cm x 1 cm of marbled tissue. Histology showed a loss of myocytes with fatty tissue replacement and vacuolated Purkinje cells. There was collagenous tissue with stippled fibroblasts.[9]

Non-invasive treatments include restraint from strenuous exercise, use of beta blockers and anti-arrhythmic medications. Surgical options include placement of an implantable cardioverter defibrillator, catheter ablation of the affected heart tissue or heart transplantation.[16]

The mouse models have been generated including mutations for desmoplakin, plakophilin-2, desmoglein-2, desmocollin-2, plakoglobin and laminin receptor-1. Mouse models might provide insight if a gene mutation alters demise adhesion or is the loss of signaling pathways that are the first step in the it of myocytes. A JUP deficient mouse mimics the pathology experienced by endurance athletes. The mutant mice subjected to endurance training had evidence of ARVC four months earlier than their untrained cohorts. These mice had right ventricular dilation without the fibrofatty replacement.[14]

The findings in this case are consistent with right heart failure - ascites, pleural effusion, peripheral edema and chronic passive hepatic congestion. The right heart failure was due to significant loss of myocytes and infiltration of adipocytes and dilatation of the right ventricle. The appearance of the heart was similar to a rare condition in humans - AVRC.

**Contributing Institution:**
National Institutes of Health
Bethesda, MD 20892
https://www.ors.od.nih.gov/sr/dvr

**JPC diagnosis:**
Heart: Fibrofatty infiltration, focally extensive, severe, with cardiomyocyte degeneration, atrophy, and hypertrophy, karyomegaly, and endocardial and myocardial fibrosis.

**JPC comment:**
The contributor provides a concise summary of ARVC. A recent investigation into the death of an alpha male bonobo included genetic sequencing and analysis. There were no

sufficiently variant sequences across 10 ARVC-associated genes (*LMNA*, *CTNNA3*, *DES*, *TGFB3*, *JUP*, *TMEM43*, *PKP2*, *DSC2*, *DSG2*, and *DSP*), but there were two variants of uncertain clinical significance in *CTNNA3* and *JUP* that were not found in controls. It is currently not known whether these fully explain this bonobo's phenotype, but it may lead to additional research.[2]

Research into (human) diagnostics have recently focused on the identification of anti-cardiac desmoglein 2 (DSG2) autoantibodies. Desmoglein-2 is a cardiac cadherin protein that provides mechanical attachment between cells. Results showed that anti-DSG2 antibodies were specific to patients with ARVC, with no anti-DSG2 antibodies detected in controls without ARVC. Additionally, disease severity positively correlated with antibody level in these patients. Research into domestic species may find an equally suitable biomarker for this disease.[3]

A differential for ARVC in human literature is cardiac sarcoidosis, which is more typically characterized by granulomatous inflammation in the myocardium, often with giant cells and accompanied by lymphoplasmacytic inflammation. However, there are numerous presentations, depending on the progression of the disease at the time of diagnosis. Clinically, because there is disruption of Purkinje fibers, this condition may mimic ARVC and manifest with AV block, dysrhythmias, or sudden cardiac death. In cardiac sarcoidosis, granulomas form irregular, infiltrating yellow-tan, white-tan, or gray lesions and may involve any part of the heart. It has also been observed that when cardiac sarcoidosis presents as ARVC, endomyocardial biopsies are characterized by fibrofatty replacement without evidence of granulomatous inflammation.[17]

During conference discussion, it was noted between participants that there was some mild slide variation, with some sections having a mild endocarditis as well. The moderator emphasized the desmosome's role in intercalated disks, and enumerated some of the documented genetic mutations in genes affecting components of desmosomes and intercalated disks in many cases of ARVC.

**References:**


1. Basso C, Fox PR, Meurs KM, et al. Arrhythmogenic right ventricular cardiomyopathy causing sudden cardiac death in boxer dogs: a new animal model of human disease. *Circulation*. 2004 Mar 9;109(9):1180-5
2. Celestino-Soper PBS, Lynnes TC Zhang L, et al. Genetic analyses in a bonobo (*Pan paniscus*) with arrhythmogenic right ventricular cardiomyopathy. *Sci Rep*. 2018;8(1):4350.
3. Chatterjee D, Fatah M, Akdis D, et al. An autoantibody identifies arrhythmogenic right ventricular cardiomyopathy and participates in its pathogenesis. *European Heart Journal*. 2018;39:3932-3944.
4. Corrado D, Thiene G, Nava A, Rossi L, Pennelli N. Sudden death in young competitive athletes: clinicopathologic correlations in 22 cases. *Am J Med*. 1990 Nov;89(5):588-96.
5. Delmar M, McKenna WJ. The cardiac desmosome and arrhythmogenic cardiomyopathies: from gene to disease. *Circ Res*. 2010 Sep 17;107(6):700-14.
6. Eason BD, Leach SB, Kuroki K. Arrhythmogenic right ventricular cardiomyopathy in a weimaraner. *Can Vet J*. 2015 Oct;56(10):1035-9.
7. Fernandez del Palacio MJ, Bernal LJ, Bayon A, Bernabé A, Montes de Oca R, Seva J Arrhythmogenic right ventricular dysplasia/cardiomyopathy in a Siberian husky. *J Small Anim Pract*. 2001 Mar;42(3):137-42.
8. Frank R, Fontaine G, Vedel J, et al. Electrocardiologie de quatre cas de dysplasie ventriculaire droite arythmogene. *Arch Mal Coeur* 1978 71:963-72.
9. Freel KM, Morrison LR, Thompson H, Else RW. Arrhythmogenic right ventricular cardiomyopathy as a cause of unexpected cardiac death in two horses. *Vet Rec*. 2010 Jun 5;166(23):718-21.
10. Harvey AM, Battersby IA, Faena M, Fews D, Darke PG, Ferasin L. Arrhythmogenic right ventricular cardiomyopathy in two cats. *J Small Anim Pract*. 2005 Mar;46(3):151-6.
11. Marcus FI, Fontaine GH, Guiraudon G, et al. Right ventricular dysplasia: a report of 24

adult cases. *Circulation*. 1982 Feb;65(2):384-98.
12. Meurs KM, Stern JA, Reina-Doreste Y, Spier AW, Koplitz SL, Baumwart RD. Natural history of arrhythmogenic right ventricular cardiomyopathy in the boxer dog: a prospective study. *J Vet Intern Med*. 2014 Jul-Aug;28(4):1214-20.
13. Oomen AWGJ, Semsarian C Puranik R, Sy RW. Diagnosis of Arrhythmogenic Right Ventricular Cardiomyopathy: Progress and Pitfalls. *Heart Lung Circ*. 2018 Apr 4. S1443-9506(18)30139-2.
14. Padron-Barthe L, Dominguez F, Garcia-Pavia P Lara-Pezzi E. Animal models of arrhythmogenic right ventricular cardiomyopathy: what have we learned and where do we go? Insight for therapeutics. *Basic Res Cardiol*. 2017 Sep;112(5):50
15. Paul M, Wichter T, Gerss J, et al. Connexin expression patterns in arrhythmogenic right ventricular cardiomyopathy. *Am J Cardiol*. 2013 May 15;111(10):1488-95.
16. Rossi P Massumi A, Gillette P Hall RJ. Arrhythmogenic right ventricular dysplasia: clinical features, diagnostic techniques, and current management. *Am Heart J*. 1982 Mar;103(3):415-20.
17. Serei VD, Fyfe B. The many faces of cardiac sarcoidosis. *Am J Clin Pathol*. 2020;153(3):294-302.
18. Vila J, Pariaut R, Moise NS, et al. Structural and molecular pathology of the atrium in boxer arrhythmogenic right ventricular cardiomyopathy. *J Vet Cardiol*. 2017 Feb;19(1):57-67

---

## CASE 3: P17-2052 (4101144-00)

**Signalment:**
13-year-old, female, Schnauzer, *Canis lupus familiaris*, dog

**History:**
The dog presented a diagnosis of intracranial neoplasia (extra-axial lesion in the olfactory and right frontal lobe area). The patient suffered from seizures and due to the worsening of clinical signs the dog was humanely euthanized and submitted for postmortem examination.

**Gross Pathology:**
Arising from the right frontal lobe and at the base of the right olfactory bulb, an irregular, firm, white, partially delimited mass with an irregular, surface measuring 1.9 x 1.2 x 2.7 cm was observed. The left frontal lobe was slightly concave by compression of the neoplasm. On cross-sections, the tissue was found occupying and partially replacing both the gray and white matter and its inner surface was well delineated, white to gray, and solid with multiple whitish areas of mineralization.

Other relevant findings were observed in the reproductive tract, where numerous cysts arising from both ovaries were present, as well, as marked endometrial cystic hyperplasia from both uterine horns.

**Laboratory results:**
None

**Microscopic description:**
Brain, right frontal lobe: Histologically, there is a proliferation of a well circumscribed, densely cellular neoplasm supported by a thin fibrovascular stroma into nests of closely packed predominantly epithelioid cells or spindle to polygonal cells arranged in loosely interlacing streams and numerous whorls. Neoplastic cells have variably distinct borders with varying amounts of eosinophilic cytoplasm, oval to

*Cerebrum. Overlying and compressing the right olfactory bulb, there is an irregular, firm, white, neoplasm with an irregular, surface measuring 1.9 x 1.2 x 2.7 cm (Photo courtesy of: Departamento de Patología, Facultad de Medicina Veterinaria y Zootecnia, Universidad Nacional Autónoma de México, Mexico City, Mexico, http://fmvz.unam.mx/fmvz/departamentos/patologia/acerca.html)*

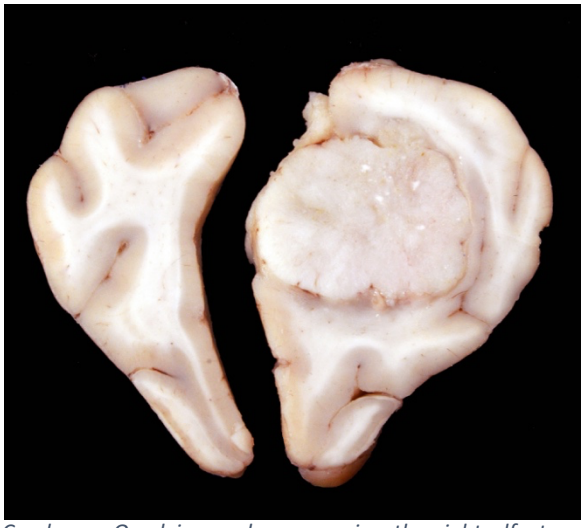

*Cerebrum. Overlying and compressing the right olfactory bulb, there is an irregular, firm, white, neoplasm with an irregular, surface measuring 1.9 x 1.2 x 2.7 cm. (Photo courtesy of: Departamento de Patología, Facultad de Medicina Veterinaria y Zootecnia, Universidad Nacional Autónoma de México, Mexico City, Mexico, http://fmvz.unam.mx/fmvz/departamentos/patologia/acerca.html)*

spindle-shaped vesicular nuclei with finely stippled chromatin and predominantly one large distinct nucleolus. Mitoses are rare with less than one mitotic figure per high power field. There is moderate anisocytosis and anisokaryosis. In the core of some whorls, there are multiple basophilic and concentric concretions consistent with areas of mineralization (Psamomma bodies), as well as areas with dystrophic mineralization.

**Contributor's morphologic diagnosis:**
Brain, right frontal lobe: Psammomatous meningioma.

**Contributor's comment:**
This case had a classic presentation and microscopic features for canine meningioma. In dogs, intracranial meningiomas account for 33% to 49% of all primary brain tumors and are the most common central nervous system (CNS) tumor in this species.[1,4,8,9] They occur predominantly beyond middle age, and there is no gender predilection in contrast to their human counterparts, where their presentation in females is more common.[4] Most meningiomas are benign. In dogs, they are more common in the brain than in the spinal cord and their development in retrobulbar sites is uncommon. The intracranial meningiomas have favored localizations. They are regularly attached to the dura mater and commonly found in the region of the olfactory bulb and frontal lobes, as observed in this case. Other locations include below the brain stem, the midline attached to the falx cerebri, or the tentorium cerebelli or an intraventricular location associated with choroid plexus.[1,4] Their attachment to the dura or leptomeninges may be broad, narrow or total (forming plaque-like masses).[4] The main initial clinical sign associated with forebrain meningiomas in dogs is seizures, opposed to cats, where the most common initial clinical signs are lethargy and behavior changes.[1] Canine meningiomas show a remarkable biological similarity to their human counterparts, therefore, the grading system in humans (WHO classification system), is commonly used to classify these tumors. The histological subtypes are summarized in table 1. Mixtures of the various forms are common.[4] Besides the histologic subtypes, the WHO CNS classification includes a grading scheme that is a malignancy scale based on specific cytological features. In humans, WHO grade is one component of a combination of criteria used to predict a response to therapy and outcome. Other criteria include the age of the patient, neurologic performance status, tumor location, radiological features such as contrast enhancement, extent of surgical resection, proliferation indices, and genetic alterations. For each tumor entity, combinations of these parameters contribute to an overall estimate of prognosis.[4,6,7]

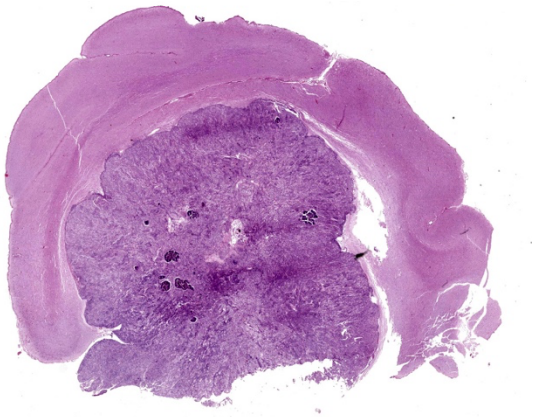

*Cerebrum, dog. A transverse section of the right telencephalic cerebral cortex containing an expansile neoplasm is presented for examination. (HE, 69X)*

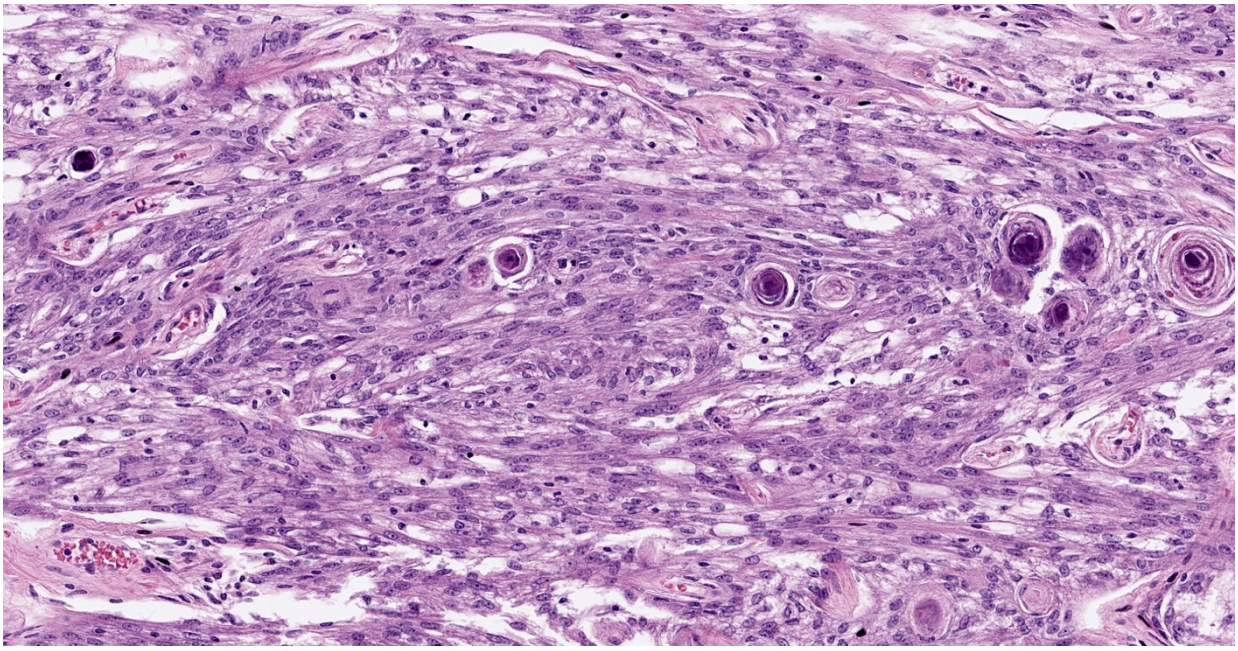

*Cerebrum, dog. Neoplastic cells are spindled, arranged in variably-sized streams and bundles with occasional whorls. The whorls often contain crystalline mineral. (HE, 216X)*

Canine meningiomas are commonly immunoreactive to vimentin intermediate filaments, cytokeratin and E-cadherin, while being immune-negative to GFAP.

In one study in dogs, incidence of atypical meningiomas was higher compared to their counterparts in humans. Psammomatous meningioma (PMs) had an incidence of 3.5% of the total meningiomas and there were no associations among tumor subtypes or grades or features in magnetic resonance imaging, but microscopically parenchymal edema primarily affecting the white matter was a common feature.[8]

In humans, intracranial PMs are also a rare subtype of meningioma with low tendency toward growth and recurrence. Intraspinal PMs are more common than intracranial PMs. Most intracranial PMs exhibit highly calcified imaging characteristics, which can be detected by computed tomography. Calcification of intraspinal PM complicates the operative procedure, because of adhesions to the spinal cord, hard tumor consistency and neurovascular structure encasement.[5] These features have not been reported in canine or feline meningiomas.

Psammoma bodies (PBs) are concentric lamellated calcified concretions, observed most commonly in several neoplasms like meningioma, papillary thyroid carcinoma, and papillary serous cystadenocarcinoma of ovary

| WHO grade | Histologic subtypes | Criteria |
|---|---|---|
| Grade 1 subtype<br><br>"Benign" | 1. Meningothelial<br>2. Fibrous (fibroblastic)<br>3. Transitional (mixed)<br>4. Psammomatous<br>5. Angiomatous<br>6. Microcystic<br>7. Secretory | Criteria not met for grades 2 or 3. |
| Grade 2 subtype<br><br>"Atypical" | 1. Chordoid<br>2. Clear cell<br>3. Atypical | Mitotic count of at least 4 mitoses/10 HPF<br>Loss of normal architecture (whorls or fascicles) and patternless cell sheets<br>Small cell formation with a high nuclear:cytoplasmic ratio<br>Nuclear atypia or macronuclei<br>Hypercellularity<br>Spontaneous necrosis<br>Brain invasion |
| Grade 3 subtype<br><br>"Anaplastic" | 1. Papillary<br>2. Rhabdoid Anaplastic | Extreme cellular anaplasia<br>Mitotic count of > 20 mitoses/10 HPF<br>Abnormal mitotic figures<br>Necrosis<br>Brain invasion |

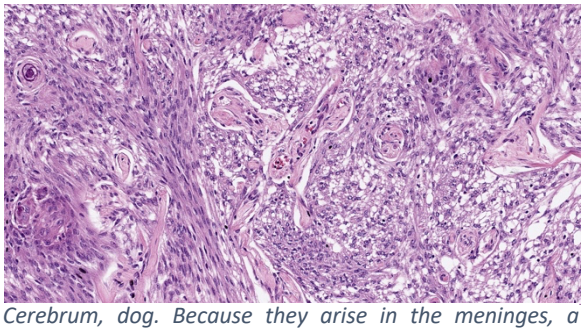

*Cerebrum, dog. Because they arise in the meninges, a variably dense fibrous stroma may be seen in meningiomas. (HE, 216X)*

and other non-neoplastic lesions. Their formation remains poorly understood, but two major hypotheses have been described. The first one attributes the formation of PBs to degeneration and necrosis of neoplastic cells and subsequent dystrophic calcification. In the second one, PBs formation is considered an active biologic process involving secretion of collagen and membrane bound vesicles in alternate layers by neoplastic cells and the calcification of vesicles, ultimately leading to degeneration/death of tumor cells and growth retardation of the neoplasm that may also serve as a barrier against its spread.[3]

**Contributing Institution:**
Departamento de Patología
Facultad de Medicina Veterinaria y Zootecnia
Universidad Nacional Autónoma de México
Mexico city, Mexico
http://fmvz.unam.mx/fmvz/departamentos/patologia/acerca.html

**JPC diagnosis:**
Cerebrum: Meningioma, grade 1, microcystic, with psammoma bodies, and chondroid and osseous metaplasia.

**JPC comment:**
The contributor summarizes canine meningioma well. While most canine meningiomas are grade I (56%), numerous cases are grade II (46%). Approximately 1% are documented as grade III meningiomas. Though varying in histologic patterns, many meningiomas exhibit early loss of tumor suppressor genes *NF2*, *4.1B*, and *TSLC1*.[2]

Additional considerations for cases of meningeal disease may include meningeal sarcomatosis. While it usually presents in the lumbar spinal cord and is infiltrative rather than expansile, neoplastic cells are pleomorphic, may extend the length of the spinal cord and be found circumferentially in the arachnoid space. In contrast to a meningioma, these neoplastic cells most often stain negative for cytokeratin.[2]

In the dog, boxers and golden retrievers have a higher incidence of meningioma, but this tumor has also been reported frequently in cats, and in horses, cattle, pigs, and wildlife to a lesser extent.[4] Meningiomas have been reported in Bactrian camels, the short beaked common dolphin, as well as a collared brown lemur.[11] Less frequent than the previously described types of meningiomas, granular cell meningiomas have been described in humans and domestic animals. In addition to intracranial meningiomas, extracranial meningiomas have been reported in dogs and humans, with the spinal cord, orbital, paranasal, and cutaneous locations most common. In an investigation of two cases of canine cutaneous meningioma, neoplastic cells were immunopositive for vimentin, but immunonegative for cytokeratin, and neurofilament, and scattered immunopositivity for S-100.[9] This may showcase the degree to which neoplastic cell protein expression depends on the microenvironment.

Standardization of neoplasm reporting provides an opportunity for the profession to truly perform more accurate statistical analyses and determine whether our current grading frameworks correlate with clinical outcomes, or whether they require revision. During discussion, the

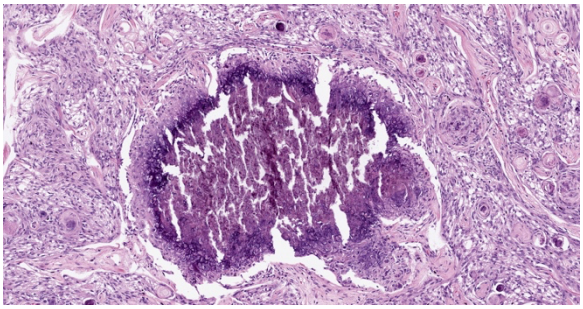

*Cerebrum, dog. Mineralized areas "psammoma bodies" are often present in areas where neoplastic cells whorl and may coalescing into large areas of crystalline mineral ranging up to 0.75mm in diameter.*

moderator emphasized that saying "less than 1 mitotic figure per…" does not represent an accurate, discrete fact about the neoplasm. If no mitotic figures are observed, state that in the report. There may be slight variation between pathologists, as it is unlikely they will evaluate the exact same 2.37 $mm^2$ area, but variations should be small. The canine meningioma grading scheme is derived from human literature and is outdated.

**References:**


1. Adamo PF, Forrest L, Dubielzig R, Canine and Feline Meningiomas: Diagnosis,Treatment, and Prognosis. Compendium. 2014; 951-956.
2. Cantile C, Youssef S. Nervous system. In: Maxie, MG, ed. *Jubb, Kennedy, and Palmer's Pathology of Domestic Animals,* Vol I. 6th ed. Philadelphia, PA: Elsevier Ltd; 2016:396-398, 494.
3. Das DK. Psammoma Body: A Product of Dystrophic Calcification or of a Biologically Active Process That Aims at Limiting the Growth and Spread of Tumor? Diagnostic Cytopathology. 2009; 37(7); 534-541.
4. Higgins RJ., Bollen AW, Dickinson PJ, Sisó-Llonch S.: Tumors of the Nervous System. In: *Tumors in Domestic Animals*, ed. Meuten DJ, 5th ed., pp. 864-869. John Wiley & Sons Inc., Iowa, Ames, 2017.
5. Lin Z, Zhao M, Ren X, Wang J, Li Z, Chen X , Wang Y, Li X, Wang C, Jiang Z. Clinical Features, Radiologic Findings, and Surgical Outcomes of 65 Intracranial Psammomatous Meningiomas. World Neurosurg. 2017; 100:395-406.
6. Louis DN, Ohgaki H, Wiestler OD, et al. The 2007 WHO classification of tumours of the central nervous system. Acta Neuropathol (Berlin) 2007;114:97–109.
7. Louis DN, Perry A, Reifenberger G, Deimling A, Figarella-Branger D, Cavenee WK, Ohgaki H, Wiestler OD, Kleihues P, Ellison DW. The 2016 World Health Organization Classification of Tumors of the Central Nervous System: a summary. Acta Neuropathol. 2016.
8. Sturges BK, Dickinson PJ, Bollen AW, Koblik PD, Kass PH, Kortz GD, Vernau KM, Knipe MF., LeCouteur RA, Higgins RJ. Magnetic Resonance Imaging and Histological Classification of Intracranial Meningiomas in 112 Dogs. J Vet Intern Med. 2008;22:586–595.
9. Summers B, Cummings J, deLahunta A: Tumors of the central nervous system, in Summers BA, Cummings JF, de Lahunta A (eds): *Veterinary Neuropathology*. St Louis, Mosby, 1995, pp 351–401.
10. Teixiera LBC, Pinkerton ME, Dubielzig RR. Periocular extracranial cutaneous meningiomas in two dogs. *Journal of Veterinary Diagnostic Investigation*. 2014;26(4):575-579.
11. Terio KA, McAloose D, St. Leger J, eds. *Pathology of Wildlife and Zoo Animals*. San Diego, CA: Elsevier. 2018; 193, 550, 339.e12.


---

## CASE 4: 50365 (4153012-00)

**Signalment:**
7-year-old, female spayed, domestic shorthair cat (*Felis catus*)

**History:**
The cat presented with a several day history of inappetence and progressive tetra-ataxia. Supportive treatment was initiated. An evaluation by the Neurology department was suggestive of left central vestibular disease. An MRI was obtained, which showed an expansile soft tissue mass extending from the nasal cavity, through the cribriform plate and into the frontal sinuses and brain. A marked mass effect with trans-tentorial and foramen magnum brain herniation was observed.

**Gross Pathology:**
Respiratory: The nasal cavity has a white, firm, gelatinous mass that measures 2 x 1 x 1 cm and is most prominent on the left side. Impression smears are obtained.

Nervous: The left frontal lobe of the brain has a focal, firm, white, gelatinous mass communicating with the nasal cavity that measures approximately 1.5 x 1.0 x 1.0 cm. The regional gyri are expanded (edema). The cerebellar vermis is markedly flattened and is visible through the foramen magnum. Upon removal of the calvarium, the vermis is markedly compressed and elongate (cerebellar coning; transforaminal herniation). Mild indentation of

the occipital lobes is observed (presumed trans-tentorial herniation).

**Laboratory results:**
Three impression smears of the left frontal lobe/nasal mass are examined. All samples are highly cellular and contain clusters of cells forming occasional acinar-like structures upon a background of amphophilic to basophilic (mucinous) material and peripheral blood. The cells are round to oval, with mild to moderate pleomorphism, and moderate amounts of basophilic cytoplasm. Many cells do not contain cytoplasm. Nuclei contain prominent single or multiple nucleoli. Occasional mitoses are found.

**Microscopic description:**
One section each from the rostral brain and nasal cavity contains a similar neoplastic process. The masses are well demarcated but infiltrative, densely cellular and comprised of neoplastic cells forming sheets, acini, rosettes and pseudorosettes amongst a scant fibrovascular stroma. The rosettes in some cases have a distinct lumen (Flexner-Wintersteiner); others contain fibrillar cytoplasmic processes (Homer-Wright) (brain), (nasal cavity). Less frequent perivascular pseudorosettes are observed. Neoplastic cells are round, oval and cuboidal to columnar, with scant to moderate amounts of eosinophilic cytoplasm and round to oval central or basilar nuclei. Nuclei contain moderately coarse chromatin and an indistinct or single central nucleolus. In regions

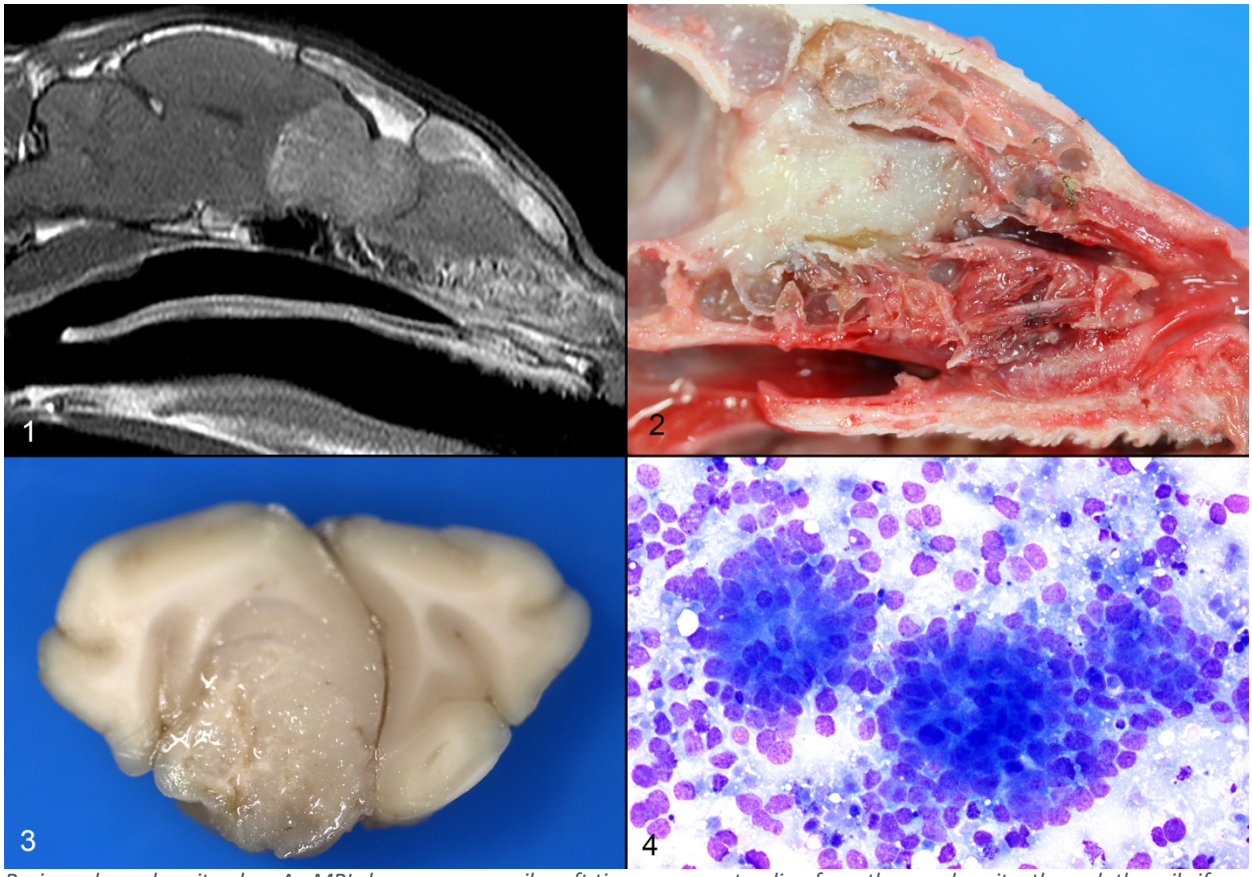


*Brain and nasal cavity, dog. An MRI shows an expansile soft tissue mass extending from the nasal cavity, through the cribriform plate and into the frontal sinuses and brain (Figure 1). The nasal cavity has a white, firm, gelatinous mass that measures 2 x 1 x 1 cm and is most prominent on the left side (Figure 2). The left frontal lobe of the brain has a focal, firm, white, gelatinous mass communicating with the nasal cavity that measures approximately 1.5 x 1.0 x 1.0 cm (Figure 3). An impression smear of the left frontal lobe/nasal mass is highly cellular and contain clusters of cells forming occasional acinar-like structures upon a background of amphophilic to basophilic (mucinous) material and peripheral blood (Figure 4). Three impression smears of the left frontal lobe/nasal mass contain clusters of cells forming occasional acinar-like structures upon a background of amphophilic to basophilic (mucinous) material and peripheral blood (Figure 4). (Photos courtesy of:* ***Animal Medical Center*** *https://www.amcny.org/)*

with the highest mitotic activity, there are greater than 100 mitoses in an area of 2.37mm$^2$ (10 high power fields with a 40x objective, 10x ocular FN 22mm, FOV diameter 0.55 mm).[3] Multifocal to coalescing necrosis is scattered throughout the neoplastic populations in both locations, with regional nuclear pyknosis and karyorrhectic debris. Mineralized vessels are observed in the brain sections. In the adjacent brain parenchyma, there are variable amounts of rarefaction with increased numbers of glial cells, including gemistocytic astrocytes and Gitter cells. In these regions, small caliber vessels are prominent with increased branching, endothelial hypertrophy and loosely separated white matter (edema). Few scattered perivascular lymphocytes and plasma cells are observed. In the leptomeninges of the surrounding brain, small populations of inflammatory cells are present, including lymphocytes and plasma cells.

In the nasal cavity, inflammatory cells are present adjacent to the mass, including numerous neutrophils with fewer foamy macrophages, lymphocytes, plasma cells and occasional lymphoid follicle formation. The turbinate bones are irregular with reversal lines and multifocal


5

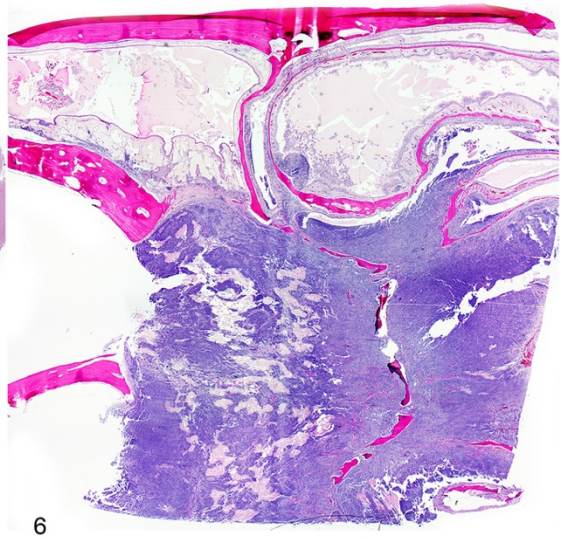
6

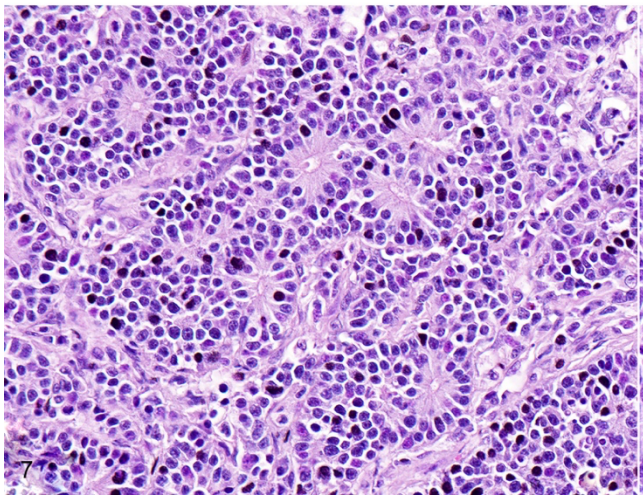
7

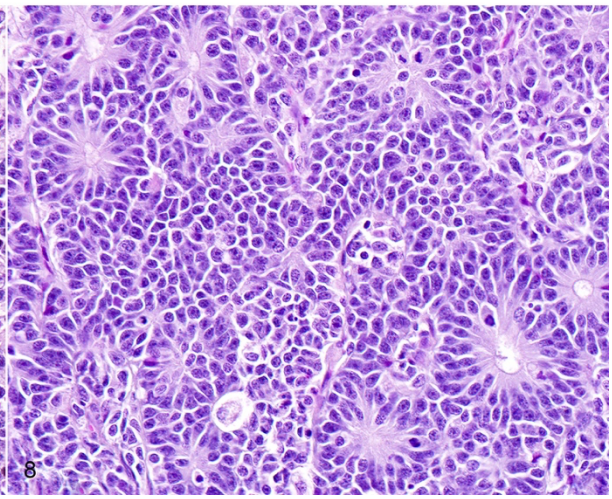
8

*Brain and nasal cavity, dog. Similar neoplasms are seen in both locations. The masses are well demarcated but infiltrative, densely cellular and comprised of neoplastic cells forming sheets, acini, rosettes and pseudorosettes amongst a scant fibrovascular stroma. There are areas of necrosis scattered throughout both masses. (Fig. 5-6). The rosettes in some cases have a distinct lumen (Flexner-Wintersteiner); others contain fibrillar cytoplasmic processes (Homer-Wright) (Figure 7 (brain), Figure 8 (nasal cavity)) (Photos courtesy of:* ***Animal Medical Center*** *https://www.amcny.org/)*

lysis with infiltration by the neoplastic populations.

**Contributor's morphologic diagnosis:**
Brain and nasal cavity: Olfactory neuroblastoma (cannot rule out neuroendocrine carcinoma) with intralesional and regional necrosis, edema, gliosis, encephalitis and rhinitis, neutrophilic, lymphoplasmacytic, moderate, chronic.

**Mitotic count:** Up to 115
**Immunohistochemistry** (brain and nasal cavity): Immunopositive for MAP-2, pancytokeratin (AE1/AE3), Synaptophysin, NSE; scant immunopositivity for NeuN, immunonegative for Chromogranin

**Contributor's comment:**
The histologic and immunohistochemical findings are supportive of a primary olfactory neuroblastoma (esthesioneuroblastoma), however, neuroendocrine carcinoma cannot be ruled out without ultrastructural evaluation or additional immunohistochemistry. This neoplasm infiltrated through the cribriform plate and into the brain, resulting in increased intracranial pressure, transforaminal and transtentorial herniation. In one case series, the most common clinical signs in dogs and cats with olfactory neuroblastoma (ONB) included unilateral epistaxis, nasal discharge, anorexia,

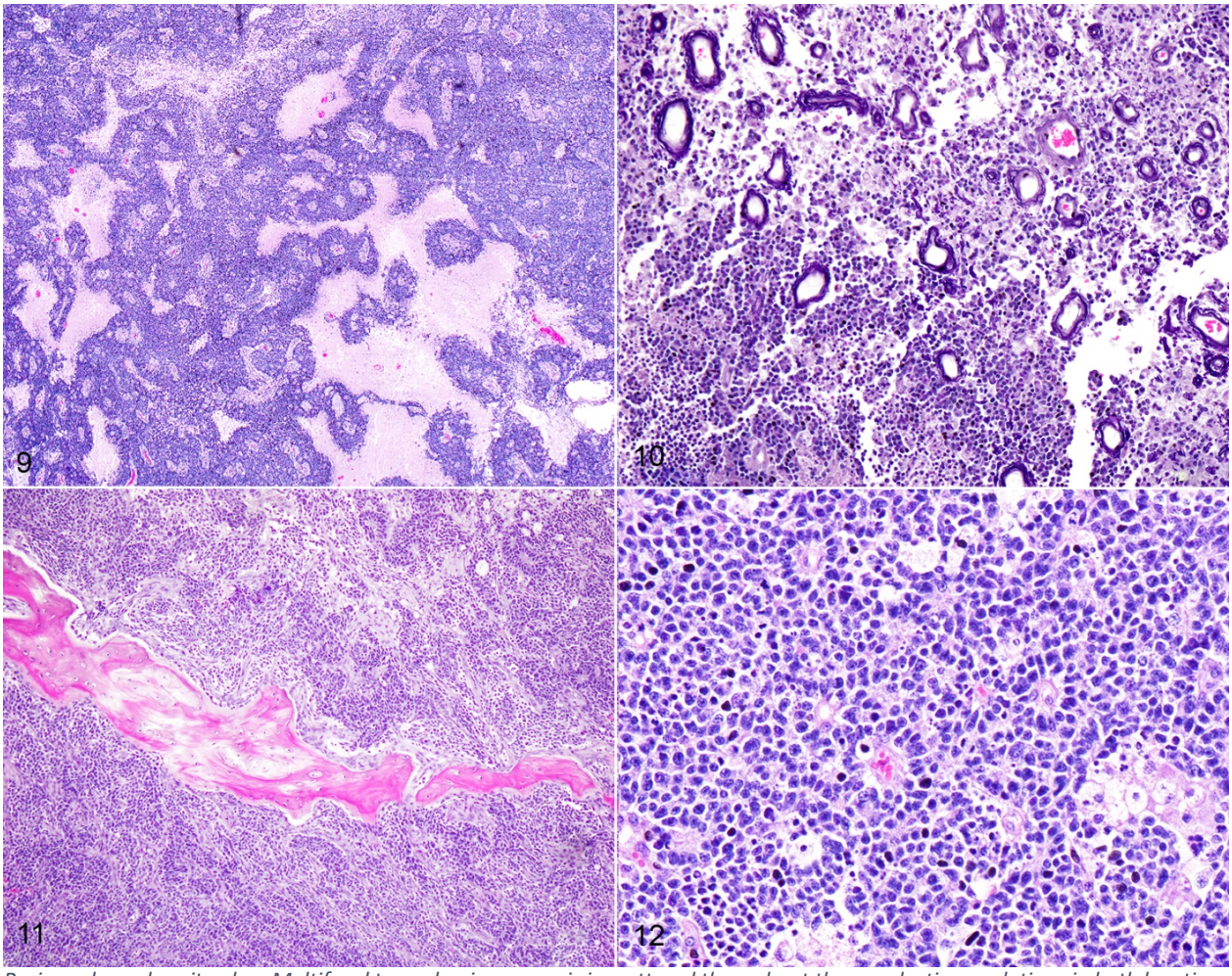


*Brain and nasal cavity, dog. Multifocal to coalescing necrosis is scattered throughout the neoplastic populations in both locations (Figures 5,6,9), with regional nuclear pyknosis and karyorrhectic debris. Mineralized vessels are observed in the brain sections (Figure 10). The turbinate bones are irregular with reversal lines and multifocal lysis with infiltration by the neoplastic populations (Figure 11). Less frequent perivascular pseudorosettes are observed (Figure 12). (Photos courtesy of:* ***Animal Medical Center*** ***https://www.amcny.org/)***

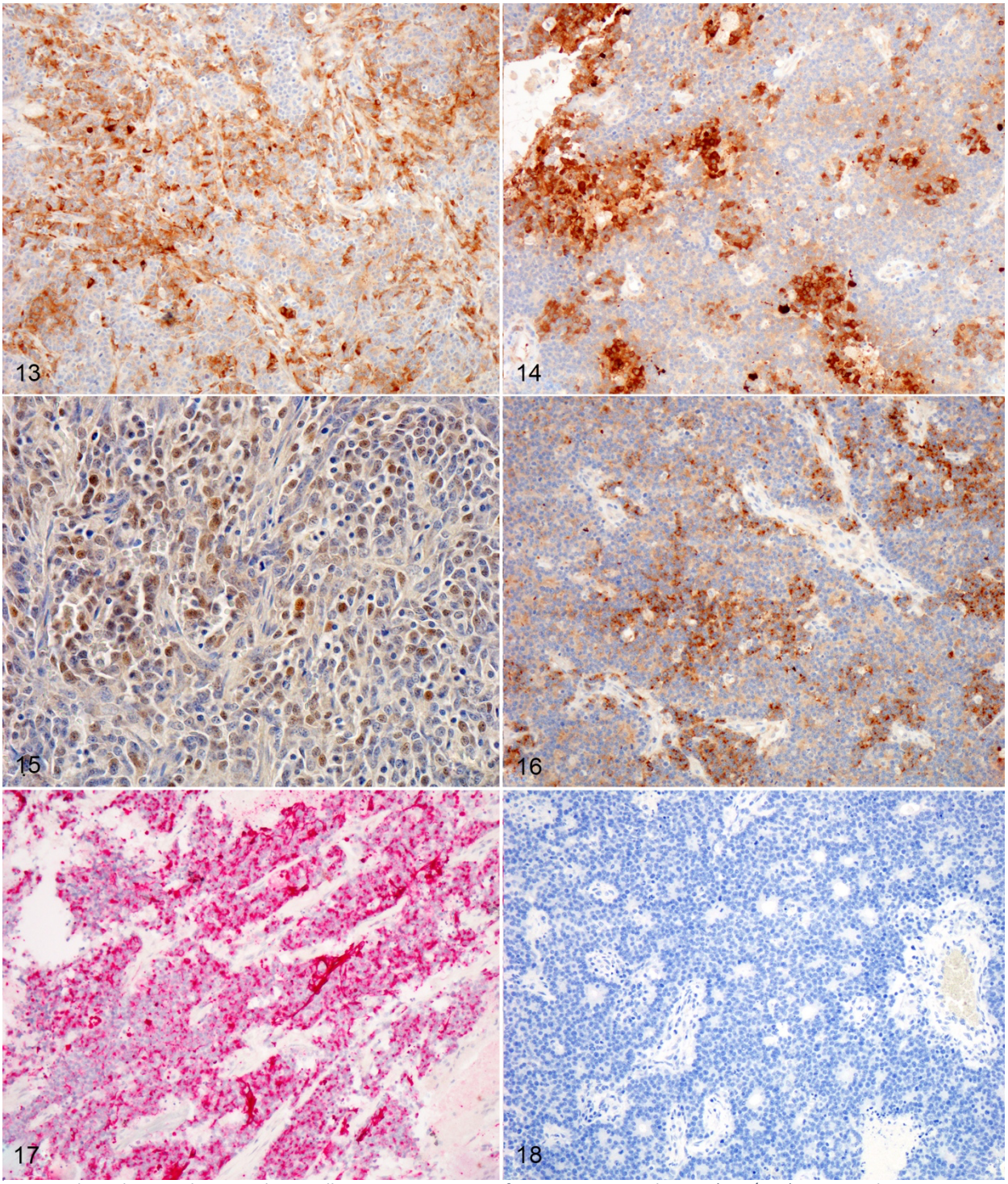


*Brain and nasal cavity, dog. Neoplastic cells are Immunopositive for MAP-2, pancytokeratin (AE1/AE3), Synaptophysin, NSE; scant immunopositivity for NeuN, immunonegative for Chromogranin (Figures 13-18) (Photos courtesy of:* ***Animal Medical Center*** ***https://www.amcny.org/)***

aggression and central nervous system (CNS) dysfunction.[1] Additional differential diagnoses include neuroendocrine carcinoma, sinonasal undifferentiated carcinoma and malignant melanoma.[1,12]

Tumors of the nasal cavity and sinuses are rare to infrequent in cats.[1,5,12] Up to 90% of feline nasal and paranasal sinus tumors are reported to be malignant.[7] Olfactory neuroblastoma (ONB) is a rare malignant neuroectodermal tumor of the nasal cavity and paranasal sinuses, thought to be derived from the olfactory neuroepithelium.[1,5,12] Olfactory neuroepithelium is present in the dorso-caudal nasal cavity and includes the rostral turbinates, cribriform plate and rostral nasal septum.[5,7] Indirect evidence suggests that these tumors may originate from olfactory stem cells.[5,8] These tumors are typically locally invasive with osteolysis and ethmoturbinate deformation.[9] Although the imaging features of this neoplasm are nonspecific, identification of a mass in the caudal nasal cavity with extension into the neurocranium are features that generate increased suspicion for ONB.[10] Metastasis to regional lymph nodes and ocular structures has been reported in domestic animals, with one case report of distant metastasis to the liver and lungs in an Afghan hound.[9] There was no evidence of metastasis in the regional lymph nodes or lungs in this case.

The histologic appearance of ONBs is varied with a spectrum of morphologic subtypes.[1,8] Well differentiated ONBs contain circumscribed lobules which are separated by a vascularized fibrous stroma with pseudorosettes and true rosettes.[1] Pleomorphism, high mitotic activity and necrosis are infrequently observed, although the latter two features are more prominent in canine and feline ONB as compared with humans.[1] Dense core neurosecretory granules and neurite-like cell processes can be observed ultrastructurally.[1]

Histologic grading (Hyam's classification in humans) is used to gauge prognosis and predict recurrence.[1] The Kadish grading scheme (a system used for staging in humans) is based upon the local spread of the neoplasm.[5] ONBs of dogs and cats were graded using the Hyam's scheme in one study and evaluated lobular architecture, nuclear pleomorphism, fibrillary matrix, rosettes, mitoses, necrosis and calcification. Grades II and III were the most common in both dogs and cats in a series of 30 cases,[1] with feline ONBs showing more differentiation and typically lower grades. Using this grading scheme, the current case would be high grade (III) due to the prominent mitotic activity and necrosis. In that case series, rosettes in feline tumors were more frequently observed than in canine tumors. This case showed frequent rosette formation.

The immunohistochemical findings support the diagnosis of ONB, however, some of the differential diagnoses cannot be entirely ruled out. In the aforementioned case series, feline cases were immunopositive for microtubule-associated protein-2 (MAP-2), Neuronal nuclei antigen (NeuN), and Neuron specific enolase (NSE).[1] In our case, neoplastic cells were positive for MAP-2, NSE, Synaptophysin, Cytokeratin, and weakly for NeuN. Neoplastic cells were diffusely negative for Chromogranin. Despite the low specificity of NSE, expression with this marker is used to support the diagnosis of olfactory neuroblastoma.[1,5] MAP-2 and NeuN are also considered reliable markers of neuronal and neuroendocrine tumors in humans.[1] In one study involving feline esthesioneuroblastoma, NeuN (a nuclear stain) did not stain central regions or cells within rosettes, a pattern which differed from that of dogs.[1] Infiltrating populations of neoplastic cells at the periphery of feline ONBs stained with NeuN, however this marker is less useful as a diagnostic marker for this neoplasm in cats.[1] The neoplastic cells in this case were diffusely immunopositive for pancytokeratin (AE1/AE2), which is typically a feature of neuroendocrine carcinoma.[12] Coexpression of NSE, Neurofilament protein (NF) and cytokeratin in human ONB has been attributed to the possible genesis from olfactory basal cells which are progenitors of olfactory receptor (neuronal) cells and sustentacular (epithelial) cells.[8] Rare expression of MAP-2 and NeuN can occur in neuroendocrine carcinomas of humans.[1] ONBs are consistently negative for epithelial membrane antigen (EMA) and carcinoembryonic antigen (CEA) which were not performed in this case due to lack of availability. Definitive differentiation would require ultrastructural evaluation or immunohistochemistry for EMA or CEA.[1,12] Both mitotic count and Ki67 labelling index (a marker of cell proliferation), were found to be much higher in feline and canine tumors as compared with human olfactory

neuroblastomas.[1] Ki-67 labelling correlated strongly with tumor grade in that study.[1,5]

FeLV has been associated with olfactory neuroblastoma, however, no causal role was established.[8] In three feline cases of spontaneous olfactory neuroblastoma, numerous mature C type retrovirus particles were identified within the tumors. Two of the three cats were serologically positive for FeLV (the third was not tested).[5,8] Olfactory neuroblastoma in humans and animals is similar with regards to morphology, ultrastructure, molecular and immunohistochemical features. Applying human staging and grading schemes may be useful for prognosticating these tumors in veterinary patients. Animal models of ONB may be helpful in the development of new treatment approaches.[5]

**Contributing Institution:**
Animal Medical Center
https://www.amcny.org/

**JPC diagnosis:**
Nasal cavity and cerebrum: Esthesioneuroblastoma (olfactory neuroblastoma).

**JPC comment:**
The contributor summarizes olfactory neuroblastoma well and illustrates the difficulty in differentiating esthesioneuroblastoma from neuroendocrine carcinoma. With H&E sections alone, it is not possible to eliminate neuroendocrine carcinoma as a potential differential diagnosis.

With an eye on improving chemotherapeutic targets, a recent retrospective analysis of 23 human olfactory neuroblastomas used DNA sequencing, whole genome RNA microarrays, gene copy number assays, and immunohistochemistry to characterize the molecular characteristics of neoplastic cells. They found that 63% of cases had genetic mutations, including *TP53*, *CTNNB1*, *EGFR*, *APC*, *cKIT*, *cMET*, *PDGFRA*, *CDH1*, *FH*, and *SMAD4*.[11] A different study found a number of olfactory neuroblastoma cells express programmed death-ligand 1 (PD-L1)[4], but this was not found in the current study. An independent study determined that 86% of studied olfactory neuroblastomas had deletions in the *Dystrophin* gene at the *DMD* locus, which is responsible for the expression of dystrophin.[3] The association between this mutation and pathogenesis is not yet clear but may warrant additional research.

Recent investigation into nine canine high-grade olfactory neuroblastomas found variable immunoreactivity of neoplastic cells to chromogranin, NF, synaptophysin, AE1/AE3 cytokeratin, and MAP2. However, all cases that were evaluated for beta-III tubulin (TuJ-1) demonstrated strong cytoplasmic immunoreactivity. Because there are overlapping immunohistochemical profiles of neuroendocrine carcinoma and olfactory neuroblastoma, TuJ-1 may represent a strong candidate for confirming a diagnosis of olfactory neuroblastoma.[2]

During discussion, the moderator emphasized the importance of standardized reporting for neoplasms. Organized reporting allows for the collection of important information that may help create future grading frameworks and allow the pathologist and clinician to provide important prognostic information to the client. The below example synoptic report was created for this case. Hopefully with standardization and collaboration, sample sizes can be pooled more easily to create statistical analyses with greater power.

| Synoptic Report Example | |
|---|---|
| **Mass size** | 2x1x1 cm (nasal) and 1.5x1x1 cm (brain) |
| **How measured** | Grossly |
| **Location** | Nasal cavity/brain |
| **MC** | Up to 115 |
| **Necrosis** | Present |
| **Histologic Grade** | Grade III (human scheme - Hyam's) |
| **Lymphovascular invasion** | Not observed |
| **Extension beyond compartment** | Yes - nasal cavity into brain |
| **How determined** | Imaging, gross histopath |
| **Diagnosis** | Olfactory neuroblastoma |
| **Ancillary tests** | IHC: Synaptophysin, NSE, MAP-2, NeuN+, Chromogranin equivocal, CEA, EMA - |
| **Metastasis** | Not documented with postmortem examination (gross and histopath) |

**References:**


1. Brosinski K et al. Olfactory neuroblastoma in dogs and cats – a histological and immunohistochemical analysis. *J comp Pathol* 2012 **146**:152-159
2. Church ME, Veluvolu SM, Durham AC, Woolard KD. Clinical outcomes,

ultrastructure and immunohistochemical features of canine high-grade olfactory neuroblastoma. *Vet Comp Oncol*. 2019;17(4):578-584.
3. Gallia GL, Zhang M, Ning Y, et al. Genomic analysis identifies frequent deletions of *Dystrophin* in olfactory neuroblastoma. *Nature Communications*. 2018;9:5410.
4. London NR, Rooper LM, Bishop JA, et al. Expression of programmed cell death-ligand 1 and associated lymphocyte infiltration in olfactory neuroblastoma. *World Neurosurgery*. 2020;135:e187-e193.
5. Lubojemska A, Borejko M, Czapiewski P, et al. Of mice and men: olfactory neuroblastoma among animals and humans. *Vet Comp Oncol*. 2016; **14**(3):e70-e82. doi:10.1111/vco.12102
6. Meuten DJ. Appendix: Diagnostic Schemes and Algorithms. In: *Tumors in Domestic Animals*, 5th ed. Meuten DJ ed. John Wiley and Sons, Inc, 2017
7. Mukaratirwa S, van der Linde-Sipman JS, Gruys E. Feline nasal and paranasal sinus tumours: clinicopathological study, histomorphological description and diagnostic immunohistochemistry of 123 cases. *J Feline Med Surg*. 2001; **3**(4):235-245. doi:10.1053/jfms.2001.0141
8. Schrenzel MD, Higgins RJ, Hinrichs SH, et al. Type C retroviral expression in spontaneous feline olfactory neuroblastomas. *Acta Neuropathol*. 1990; **80**(5):547-53.
9. Siudak K, Klinger M, Schmidt MJ, et al. Metastasizing esthesioneuroblastoma in a dog. *Vet Pathol*. 2015; **52**(4):692-695.
10. Söffler C, Hartmann A, Gorgas D, et al. Magnetic resonance imaging features of esthesioneuroblastoma in three dogs and one cat. *Tierarztl Prax Ausg K Kleintiere Heimtiere*. 2016; **44**(5):333-340. doi:10.15654/TPK-150963
11. Topcagic J, Feldman R, Ghazalpour A, Swensen J, Gatalica Z, Vranic S. Comprehensive molecular profiling of advanced/metastatic olfactory neuroblastomas. *PLOS One*. 2018;13(1): e0191244.
12. Wilson D W. Tumors of the Respiratory System. In: *Tumors in Domestic Animals*, 5th ed. Meuten DJ ed. John Wiley and Sons, Inc, 2017